

The Adiabatic Invariant of Dark Matter in Spiral Galaxies

Bruce Hoeneisen

Universidad San Francisco de Quito, Quito, Ecuador

Email: bhoeneisen@usfq.edu.ec

How to cite this paper: Hoeneisen, B. (2019) The Adiabatic Invariant of Dark Matter in Spiral Galaxies. *International Journal of Astronomy and Astrophysics*, 9, 355-367.

<https://doi.org/10.4236/ijaa.2019.94025>

Received: August 20, 2019

Accepted: September 27, 2019

Published: September 30, 2019

Copyright © 2019 by author(s) and Scientific Research Publishing Inc. This work is licensed under the Creative Commons Attribution International License (CC BY 4.0).

<http://creativecommons.org/licenses/by/4.0/>



Open Access

Abstract

Collisionless dark matter can only expand adiabatically. To test this idea and constrain the properties of dark matter, we study spiral galaxies in the “Spitzer Photometry and Accurate Rotation Curves” (SPARC) sample. Fitting the rotation curves, we obtain the root-mean-square (rms) velocity and density of dark matter in the core of the galaxies. We then calculate the rms velocity $v_{\text{rms}}(1)$ that dark matter particles would have if expanded adiabatically from the core of the galaxies to the present mean density of dark matter in the universe. We obtain this “adiabatic invariant” $v_{\text{rms}}(1)$ for 40 spiral galaxies. The distribution of $v_{\text{rms}}(1)$ has a mean 0.87 km/s and a standard deviation of 0.27 km/s. This low relative dispersion is noteworthy given the wide range of the properties of these galaxies. The adiabatic invariant $v_{\text{rms}}(1)$ may, therefore, have a cosmological origin. In this case, the rms velocity of non-relativistic dark matter particles in the early universe when density perturbations are still linear is $v_{\text{rms}}(a) = v_{\text{rms}}(1)/a$, where a is the expansion parameter. The adiabatic invariant obtains the ratio of dark matter temperature $T_h(a)$ to mass m_h in the early universe.

Keywords

Spiral Galaxies, Dark Matter, Dark Matter Properties

1. Introduction

This is our motivation. Collisionless non-relativistic dark matter can only expand adiabatically conserving $v_{\text{rms}}/\rho_h^{1/3}$, where v_{rms} is the root-mean-square (rms) of the dark matter particle velocities, and ρ_h is the density of dark matter. It turns out that we are able to measure $v_{\text{rms}}/\rho_h^{1/3}$ in the core of spiral galaxies by fitting their rotation curves. In the early universe, when density pertur-

bations are relatively small, $v_{\text{rms}}(a)$ of non-relativistic dark matter can be written in the form

$$v_{\text{rms}}(a) = \frac{v_{\text{rms}}(1)}{a}, \tag{1}$$

and $\rho_h = \Omega_c \rho_{\text{crit}} / a^3$, where a is the expansion parameter. Note that the expansion is adiabatic. Consider a free observer in a density peak. The dark matter in this peak expands, reaches maximum expansion, and then contracts forming a galaxy, conserving $v_{\text{rms}} / \rho_h^{1/3}$. Let $\langle v_{\text{th}}^2 \rangle^{1/2}$ be the root-mean-square of the radial component of the dark matter particle velocities, and let $\rho_h(r \rightarrow 0)$ be the dark matter density in the core of the galaxy. Adiabatic expansion then implies that [1] [2]

$$v_{\text{rms}}(1) \equiv \sqrt{3} \langle v_{\text{th}}^2 \rangle^{1/2} \left(\frac{\Omega_c \rho_{\text{crit}}}{\rho_h(r \rightarrow 0)} \right)^{1/3}. \tag{2}$$

Note that $v_{\text{rms}}(1)$ is, by definition, the rms velocity of dark matter particles when dark matter with density $\rho_h(r \rightarrow 0)$ in the core of the galaxy is expanded adiabatically until it acquires the present mean dark matter density of the universe $\Omega_c \rho_{\text{crit}}$ [3]. We *predict* that the ‘‘adiabatic invariant’’ $v_{\text{rms}}(1)$ is the same for all relaxed, steady state, galaxies. The purpose of the present analysis is to test this prediction. Note that measuring $v_{\text{rms}}(1)$ obtains the ratio of dark matter temperature $T_h(a)$ to mass m_h in the early universe.

In this article, we present a study of the adiabatic invariant $v_{\text{rms}}(1)$ of galaxies in the ‘‘Spitzer Photometry and Accurate Rotation Curves’’ (SPARC) sample [4].

2. Spiral Galaxy Data

We analyze the publicly available data of the SPARC galaxy sample [4]. This sample contains 175 galaxies with new surface photometry at 3.6 μm , and extended rotation curves of atomic hydrogen (HI) from the literature (see individual references in [4]). Approximately one third of the galaxies also have H α rotation curves. The SPARC sample includes a very broad range of luminosities, surface brightnesses, rotation velocities, and Hubble types.

In the present analysis, we study the 99 galaxies with high-quality rotation curves, *i.e.* galaxies with quality flag $Q = 1$. We further visually examine the galaxy rotation curves, in order to guarantee sufficient data points in the flat part (to constrain $\langle v_{\text{th}}^2 \rangle^{1/2}$), and sufficient data points in the galaxy core (to constrain $\rho_h(r \rightarrow 0)$). We are interested in galaxies with a relaxed structure in a steady-state, and so, by visual inspection, remove galaxies with rotation curves with extraneous features that may indicate recent mergers, strong warps, or galaxies with multi-spin components.

The rotation velocity $v_{\text{tot}}(r) \equiv v(r)$ is by definition the velocity of a test particle in a circular orbit of radius r in the plane of the galaxy. $v(r)$ has contributions from baryons (stars in the disk and bulge, and gas), and the halo of dark

matter [4]:

$$v(r)^2 = v_b(r)^2 + v_h(r)^2, \quad (3)$$

$$v_b = \sqrt{|v_{\text{gas}}|v_{\text{gas}} + \Upsilon_{\text{disk}}|V_{\text{disk}}|V_{\text{disk}} + \Upsilon_{\text{bulge}}|V_{\text{bulge}}|V_{\text{bulge}}}. \quad (4)$$

V_{disk} and V_{bulge} are stellar contributions to the rotation velocity inferred from the $3.6 \mu\text{m}$ photometry assuming a stellar mass-to-light ratio $1M_{\odot}/L_{\odot}$. The mass-to-light ratios of stars in the disk and bulge in units of M_{\odot}/L_{\odot} are taken to be $\Upsilon_{\text{disk}} \equiv \Upsilon_{\star}$ and $\Upsilon_{\text{bulge}} = 1.4\Upsilon_{\star}$, respectively [4]. Estimates of Υ_{\star} range from 0.5 to 0.2, see the discussion in Reference [4].

3. Fits to Spiral Galaxy Rotation Curves

Examples of spiral galaxy rotation curves are presented in **Figures 1-3**. The flat rotation velocity $v(r)$ at large r determines $\langle v_{\text{th}}^2 \rangle / (1 - \kappa_h) = v_{\text{flat}}^2 / 2$. The slopes of $v(r)$ and $v_b(r)$ at small r determine

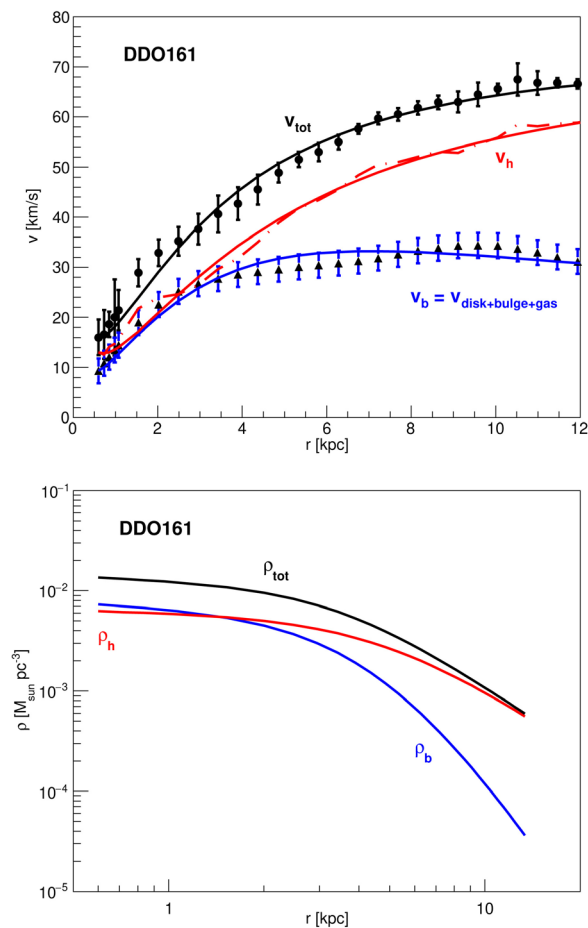


Figure 1. Top figure: Observed rotation curve $v_{\text{tot}}(r)$ (dots) and the baryon contribution $v_b(r)$ (triangles) of galaxy DDO161. The dot-dash line is from Equation (3). The solid lines are obtained by numerical integration as explained in the text. The fitted parameters are given in **Table A1** and **Table A3**. Bottom figure: Mass densities of baryons and dark matter obtained by the numerical integration. The fit obtains $\Upsilon_{\star} = 0.29 \pm 0.14$.

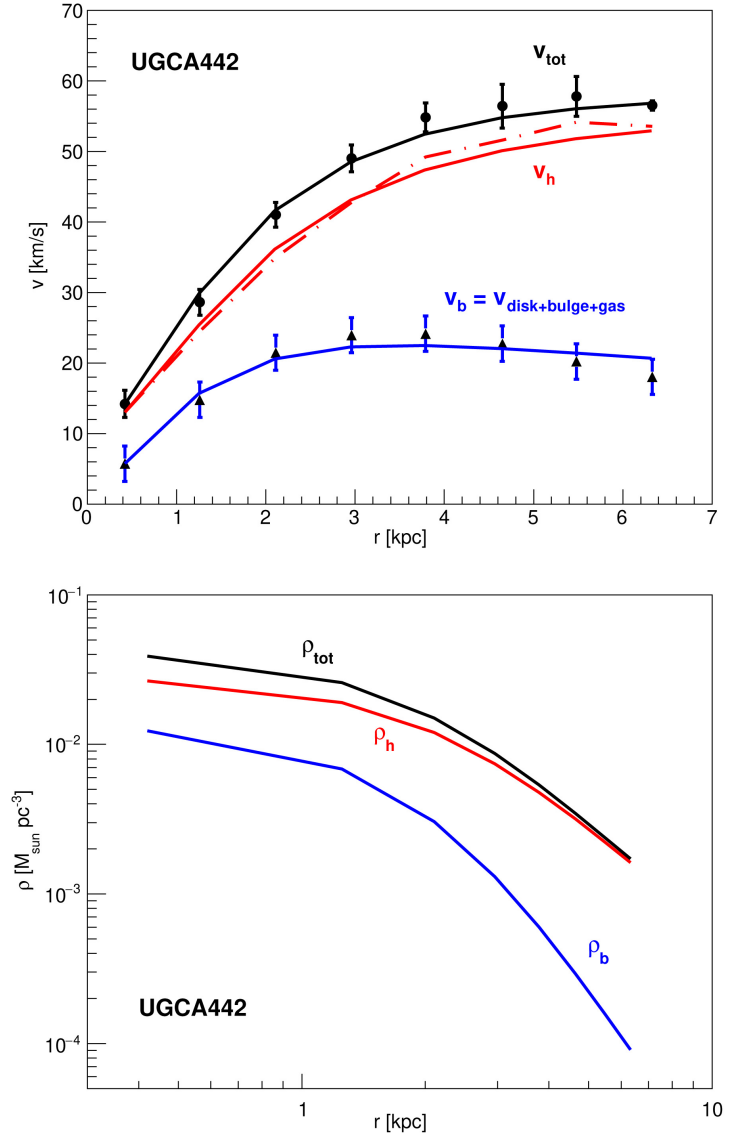


Figure 2. Top figure: Observed rotation curve $v_{\text{tot}}(r)$ (dots) and the baryon contribution $v_b(r)$ (triangles) of galaxy UGCA442. The dot-dash line is from Equation (3). The solid lines are obtained by numerical integration as explained in the text. The fitted parameters are given in **Table A1** and **Table A3**. Bottom figure: Mass densities of baryons and dark matter obtained by the numerical integration. The fit obtains $\Upsilon_* = 0.40 \pm 0.15$.

$$\rho_h(r \rightarrow 0) = 3 \left[v(r)^2 - v_b(r)^2 \right] / (4\pi G r^2).$$

κ_h is a correction to account for possible dark matter rotation.

To take full advantage of the measured rotation curves, we integrate differential equations describing two self-gravitating non-relativistic gases: baryons and dark matter, see Reference [1] for details. These differential equations require four boundary conditions: $\langle v_{th}^2 \rangle' \equiv \langle v_{th}^2 \rangle / (1 - \kappa_h)$, and $\rho_h(r_{\text{min}})$ for dark matter, and two similar parameters for baryons, where r_{min} is the radial coordinate of the first measured point. The four boundary conditions are fitted to minimize

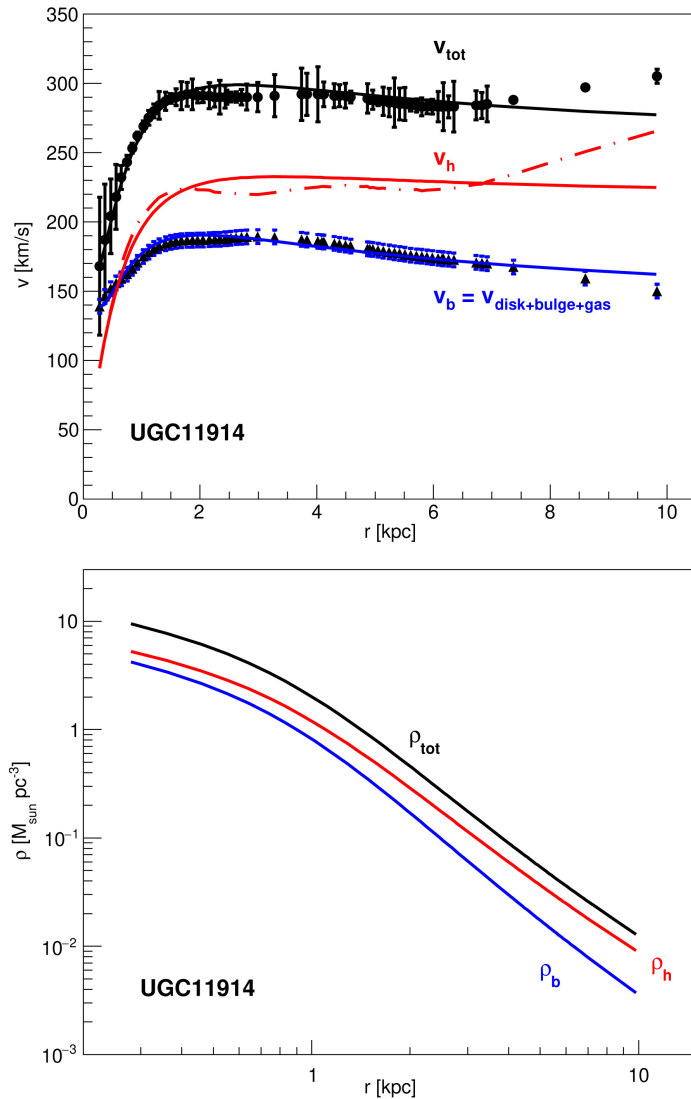


Figure 3. Top figure: Observed rotation curve $v_{\text{tot}}(r)$ (dots) and the baryon contribution $v_b(r)$ (triangles) of galaxy UGC11914. The dot-dash line is from Equation (3). The solid lines are obtained by numerical integration as explained in the text. The fitted parameters are given in [Table A1](#) and [Table A3](#). Bottom figure: Mass densities of baryons and dark matter obtained by the numerical integration. These fits have $\Upsilon_* = 0.3$ fixed.

a χ^2 between the measured rotation curves $v(r)$ and $v_b(r)$, and the corresponding calculated rotation curves. The calculated rotation curves are presented in [Figures 1-3](#) with continuous lines. Note that good fits are obtained with $\langle v_{rh}^2 \rangle'$ and $\langle v_{rb}^2 \rangle'$ taken to be independent of r . A core correction $\Delta\rho_h = \rho_h(r \rightarrow 0) - \rho_h(r_{\min})$ is obtained by extrapolation.

In Reference [1] we estimate $\kappa_b \approx 0.98$ and $\kappa_h \approx 0.15$. κ_h is model dependent and uncertain. In the present analysis, we will not consider dark matter rotation, *i.e.* we set $\kappa_h = 0$. To correct for dark matter rotation, all $v_{\text{rms}}(1)$ in this article need to be multiplied by $\sqrt{1 - \kappa_h}$.

The χ^2 of the fits requires the assignment of uncertainties to $v(r)$ and

$v_b(r)$. The uncertainties of the $v(r)$ measurements are given by the SPARC data. We generally assign $\Delta v_b(r) = \pm 3$ km/s to cover point-to-point fluctuations (this may vary in some galaxies), plus a term $(\Upsilon_* - 0.4)^2 / 0.15^2$ in the χ^2 to allow for coherent fluctuations of $v_b(r)$. The fit is accepted only if the fitted Υ_* lies in the range from 0.2 to 0.5. We set m_h to some large value, e.g. 500 eV, to avoid the onset of Fermi-Dirac or Bose-Einstein degeneracy [1]. Fits for 40 galaxies passing our default selections are presented in **Table A1** and **Table A3** in the **Appendix**. The distribution of the adiabatic invariant $v_{hrms}(1)$ for these 40 galaxies is presented in **Figure 4**. The distribution of $v_{hrms}(1)$ has a mean 0.87 km/s and a standard deviation of 0.27 km/s.

Additionally we perform fits with fixed $\Upsilon_* = 0.5$ and $\Upsilon_* = 0.2$. Finally, we perform a fit for fermions with $N_f = 2$ degrees of freedom, $m_h = 53.5$ eV corresponding to chemical potential $\mu \approx 0$ [2], free Υ_* , and $\kappa_b = 0.98$, to test the onset of Fermi-Dirac degeneracy. The distributions of the adiabatic invariant $v_{hrms}(1)$ for these additional fits are presented in **Figures 5-7** respectively.

For comparison, in **Figure 8** we present the distribution of the adiabatic invariant $v_{hrms}(1)$ of galaxies of the THINGS sample [5]. These $v_{hrms}(1)$ are taken from Table 2 of Reference [2] divided by $\sqrt{1-0.15}$ to refer the result to the case of no dark matter rotation, *i.e.* $\kappa_h = 0$, for direct comparison with the distributions of SPARC galaxies in **Figures 4-7**. Note that the method to normalize $v_b(r)$ for the SPARC and THINGS galaxy samples are different [4] [5] (see also discussion in Reference [1]). In **Figure 4**, 37 out of 40 SPARC galaxies have $\rho_h(r \rightarrow 0) > \rho_b(r \rightarrow 0)$. In **Figure 5**, 39 out of 44 SPARC galaxies have $\rho_h(r \rightarrow 0) > \rho_b(r \rightarrow 0)$. In **Figure 8**, no THINGS galaxy has $\rho_h(r \rightarrow 0) > \rho_b(r \rightarrow 0)$.

Note that fluctuations of the measured $v_{hrms}(1)$ are expected from irregularities of the rotation curves (for example, see **Figures 1-3**), as well as due to dark matter rotation, and statistical uncertainties.

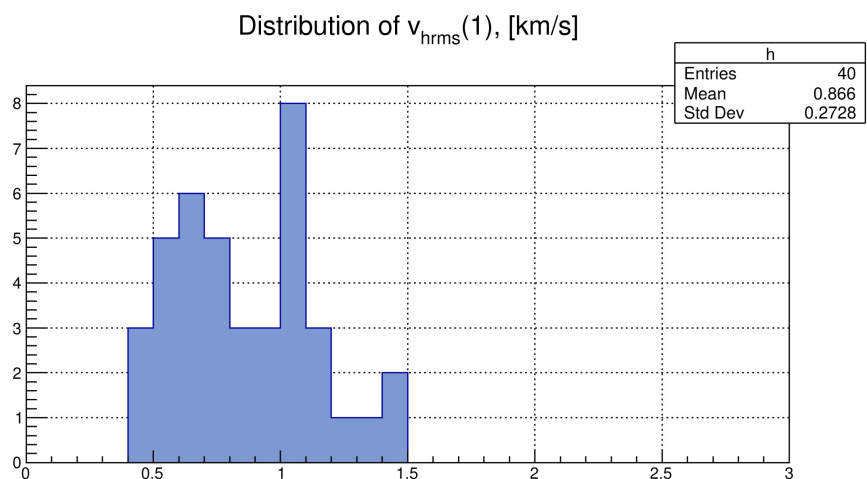


Figure 4. Distribution of the adiabatic invariant $v_{hrms}(1)$ corresponding to the fit with Υ_* free and large $m_h = 500$ eV. See **Table A1** and **Table A3** for details. Each entry has weight $w = 1$.

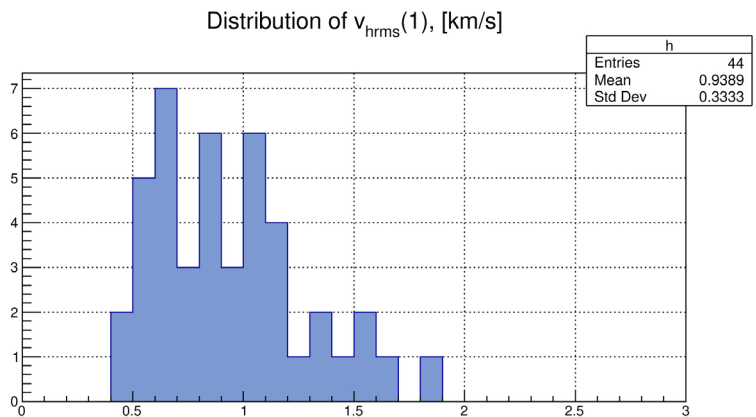


Figure 5. Distribution of the adiabatic invariant $v_{hrms}(1)$ corresponding to the fit with $\Upsilon_* = 0.5$ fixed and large $m_h = 500$ eV . See **Table A3** for details. Each entry has weight $w = 1$.

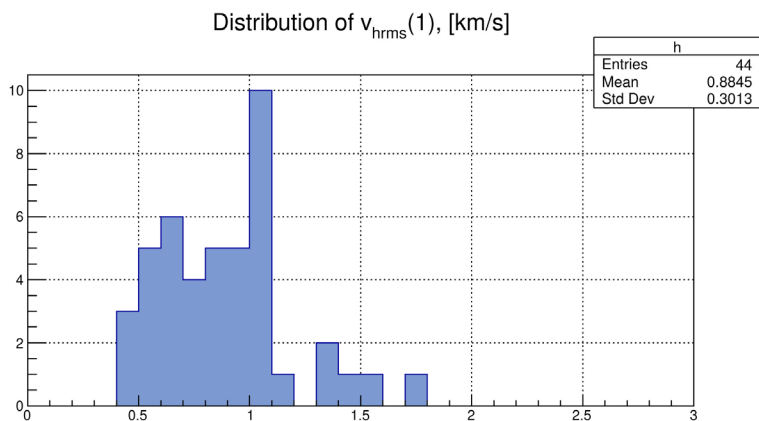


Figure 6. Distribution of the adiabatic invariant $v_{hrms}(1)$ corresponding to the fit with $\Upsilon_* = 0.2$ fixed and large $m_h = 500$ eV . See **Table A3** for details. Each entry has weight $w = 1$.

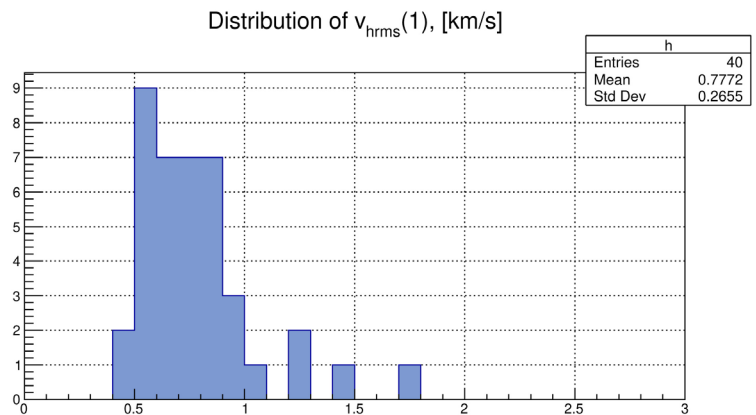


Figure 7. Distribution of the adiabatic invariant $v_{hrms}(1)$ corresponding to the fit with Υ_* free, $m_h = 53.5$ eV , $\kappa_b = 0.98$, and fermions with $N_f = 2$ degrees of freedom. This m_h corresponds to chemical potential $\mu \approx 0$ [2], to see the effect of the onset of Fermi-Dirac degeneracy. See **Table A3** for details. Each entry has weight $w = 1$.

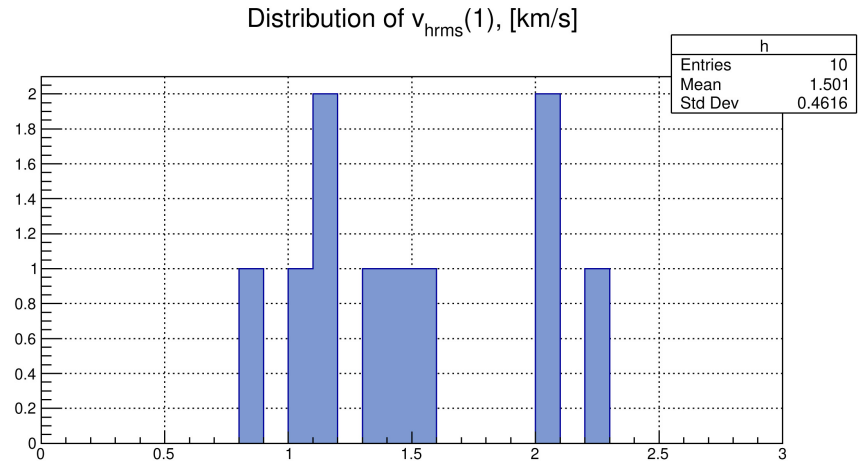


Figure 8. Distribution of the adiabatic invariant $v_{hrms}(1)$ of galaxies in the THINGS sample for the case of no dark matter rotation $\kappa_h = 0$ [2]. These galaxies are not contained in **Table A1**. Each entry has weight $w = 1$.

4. Discussion of Results

The galaxies listed in **Table A1** have absolute luminosities, central densities, and central surface brightnesses that span three orders of magnitude, and baryonic angular momenta that span five orders of magnitude. The small relative standard deviation of $v_{hrms}(1)$ is therefore noteworthy. The adiabatic invariant $v_{hrms}(1)$ does not depend significantly on the properties of the galaxies as shown in **Table 1**. These observations suggest a cosmological origin of $v_{hrms}(1)$.

5. Cosmological Implications of the Adiabatic Invariant

We consider the case of dark matter that decouples from the Standard Model sector and from self-annihilation while density perturbations are still linear. We neglect interactions of non-relativistic dark matter particles, except for gravity, or elastic dark matter-dark matter collisions. A non-relativistic gas of non-interacting particles can only expand or contract adiabatically conserving $v_{hrms} / \rho_h^{1/3}$. When dark matter particles are non-relativistic, and density perturbations are still linear, the rms velocity of dark matter particles in the expanding universe has the form

$$v_{hrms}(a) = \frac{v_{hrms}(1)}{a}, \tag{5}$$

with $v_{hrms}(1)$ given by Equation (2). In conclusion, if dark matter decouples while density perturbations are still linear, then the adiabatic invariant $v_{hrms}(1)$ given by Equation (2) should be the same for all relaxed, steady-state galaxies, independently of their history of hierarchical formation and mergers (except for a correction due to dark matter rotation).

Consider a galaxy with $v_{flat} = 300$ km/s. From the adiabatic invariant, the dark matter density in the core of this galaxy is approximately 8×10^7 times the mean dark matter density of the universe. What stopped the dark matter collapse

Table 1. Mean and standard deviation of $v_{hms}(1)$ for several galaxy selections. The default galaxy fit with free Υ_* and large $m_h = 500$ eV is used. N is the number of galaxies in the selection. $L_{3.6}$ is the absolute luminosity at 3.6 μm . M_{HI} is the mass of atomic hydrogen gas (HI). ‘‘SBdisk’’ is the Disk Central Surface Brightness at 3.6 μm . The galaxy classes are 5 = Sc, 6 = Scd, 7 = Sd, 9 = Sm, 10 = Im.

Galaxy selection	N	Mean $v_{hms}(1)$ [km/s]	Std. dev. [km/s]
All	40	0.866	0.273
$L_{3.6} < 1 \times 10^9 L_\odot$	11	0.838	0.297
$L_{3.6} > 4 \times 10^9 L_\odot$	11	1.036	0.192
$M_{HI} < 1 \times 10^9 M_\odot$	17	0.714	0.239
$\langle v_{in}^2 \rangle^{1/2} < 50$ km/s	17	0.786	0.259
$\langle v_{in}^2 \rangle^{1/2} > 60$ km/s	16	0.969	0.227
de Vaucouleurs class 5, 6 or 7	15	0.820	0.277
de Vaucouleurs class 9 or 10	18	0.869	0.258
SBdisk $< 100 \times 10^9 L_\odot / \text{pc}^2$	10	0.843	0.174
$\rho_h(0) > \rho_b(0)$	37	0.842	0.255

from reaching infinite density? Why a core and not a cusp? We consider three alternatives:

1) The collapse is ongoing. Then the distribution of $v_{hms}(1)$ would be very wide contrary to observation.

2) If $v_{hms}(1)$ is of cosmological origin, *i.e.* if $v_{hms}(1)$ is the same for all relaxed, steady-state galaxies, then a galaxy with a given $v_{\text{flat}} = \sqrt{2} \langle v_{th}^2 \rangle^{1/2}$, has a well defined dark matter density in the core $\rho_h(r \rightarrow 0)$ given by Equation (2).

3) Fermi-Dirac degeneracy of fermion dark matter may halt the collapse.

Note that $v_{hms}(a)$ in Equation (5) obtains the ratio of dark matter temperature $T_h(a)$ to mass m_h in the early universe. To obtain the mass m_h and temperature $T_h(a)$ separately, one more relation is needed, for example, the chemical potential μ of dark matter [1] [2]. We find that the particular value $\mu = 0$ is very special: it obtains a detailed, precise and consistent picture of dark matter [1] [2]. This particular value $\mu = 0$ is close to case 3, and both cases 2 [1] [2] and 3 [6] obtain similar dark matter masses m_h .

6. Conclusions

We have obtained the adiabatic invariant $v_{hms}(1)$ of 40 galaxies in the SPARC sample. The distribution of $v_{hms}(1)$ has a mean 0.87 km/s and a standard deviation of 0.27 km/s for relaxed galaxies with properties in wide ranges. This small relative standard deviation suggests a cosmological origin of $v_{hms}(1)$. If so, non-relativistic dark matter in the early universe, when density perturbations are still linear, satisfies

$$v_{\text{hrms}}(a) = \frac{v_{\text{hrms}}(1)}{a} = \sqrt{\frac{3kT_h(a)}{m_h}}. \quad (6)$$

In summary, the adiabatic invariant $v_{\text{hrms}}(1)$ obtains the ratio of dark matter temperature $T_h(a)$ to mass m_h in the early universe. Note that temperature can be assigned to dark matter because it satisfies the Boltzmann distribution [1]. The present study confirms the results obtained with galaxies in the THINGS sample [1] [2].

Conflicts of Interest

The author declares no conflicts of interest regarding the publication of this paper.

References

- [1] Hoeneisen, B. (2019) A Study of Dark Matter with Spiral Galaxy Rotation Curves. *International Journal of Astronomy and Astrophysics*, **9**, 71-96. <https://doi.org/10.4236/ijaa.2019.92007>
- [2] Hoeneisen, B. (2019) A Study of Dark Matter with Spiral Galaxy Rotation Curves. Part II. *International Journal of Astronomy and Astrophysics*, **9**, 133-141. <https://doi.org/10.4236/ijaa.2019.92010>
- [3] Tanabashi, M., *et al.* (Particle Data Group) (2018) The Review of Particle Physics. *Physical Review D*, **98**, Article ID: 030001. <https://doi.org/10.1103/PhysRevD.98.030001>
- [4] Lelli, F., McGaugh, S.S. and Schombert, J.M. (2016) SPARC: Mass Models for 175 Disk Galaxies with Spitzer Photometry and Accurate Rotation Curves. *The Astronomical Journal*, **152**, 157. (The Data in Digital Form Is Publicly Available in Files SPARC Lelli2016c.mrt and LTG data.txt) <https://doi.org/10.3847/0004-6256/152/6/157>
- [5] de Blok, W.J.G., *et al.* (2008) High-Resolution Rotation Curves and Galaxy Mass Models from THINGS. *The Astronomical Journal*, **136**, 2648-2719. <https://doi.org/10.1088/0004-6256/136/6/2648>
- [6] Hoeneisen, B. (1993) *Thermal Physics*. Mellen Research University Press, San Francisco.

Appendix: Fits to Spiral Galaxy Rotation Curves

Table A1. Fitted parameters with free Υ_* and large $m_h = 500 \text{ eV}$. Entries with an * obtain fitted Υ_* outside of the range from 0.2 to 0.5. For these entries, we show the fit with $\Upsilon_* = 0.2$ or $\Upsilon_* = 0.5$ fixed, whichever has smaller χ^2 . Uncertainties are statistical at 68% confidence as returned by the fitter. Correlations are presented in Reference [1]. The correction $\Delta\rho_h \equiv \rho_h(r \rightarrow 0) - \rho_h(r_{\min})$ is obtained by extrapolation.

Galaxy	$\langle v_{\text{th}}^2 \rangle^{1/2}$	$\langle v_{\text{th}}^2 \rangle^{1/2}$	$\rho_h(r_{\min})$	$\rho_b(r_{\min})$	r_{\min}	$\Delta\rho_h$
	[km/s]	[km/s]	[$10^{-2} M_{\odot} \cdot \text{pc}^{-3}$]	[$10^{-2} M_{\odot} \cdot \text{pc}^{-3}$]	[kpc]	[same]
D631-7	49.8 ± 4.4	21.2 ± 1.1	1.04 ± 0.12	1.59 ± 0.39	0.45	0.00 ± 0.00
DDO064	34.9 ± 5.8	40.8 ± 9.3	4.49 ± 1.23	1.13 ± 0.37	0.10	0.00 ± 0.00
DDO161	48.7 ± 1.5	32.5 ± 1.1	0.62 ± 0.05	0.76 ± 0.15	0.60	0.00 ± 0.00
ESO116						
-G012	73.9 ± 3.7	57.4 ± 3.9	6.26 ± 1.32	3.71 ± 1.94	0.25	0.00 ± 0.00
F563-1	66.7 ± 2.2	83.9 ± 7.2	4.62 ± 0.81	0.21 ± 0.07	1.07	0.50 ± 0.50
F563-V2*	72.8 ± 4.4	85.0 ± 7.5	10.88 ± 2.65	1.11 ± 0.28	0.28	0.00 ± 0.00
F568-1	80.3 ± 3.5	190.5 ± 86.3	7.12 ± 1.44	0.16 ± 0.08	0.44	0.00 ± 0.00
F568-3	68.0 ± 3.2	79.7 ± 10.2	2.05 ± 0.22	0.25 ± 0.13	0.64	0.00 ± 0.00
F568-V1	70.1 ± 3.1	88.2 ± 14.8	9.44 ± 2.02	0.42 ± 0.37	0.39	0.00 ± 0.00
F571-8*	99.9 ± 2.7	40.6 ± 1.0	4.44 ± 0.42	14.60 ± 2.08	0.22	0.00 ± 0.00
F574-1*	60.0 ± 1.4	65.8 ± 3.3	4.52 ± 0.61	0.75 ± 0.11	0.47	0.00 ± 0.00
F579-V1	69.5 ± 2.3	87.7 ± 6.2	21.17 ± 5.36	1.28 ± 0.77	0.42	2.00 ± 1.00
F583-1	51.5 ± 2.1	99.5 ± 20.8	2.21 ± 0.22	0.09 ± 0.03	0.26	0.00 ± 0.00
F583-4	40.4 ± 2.1	38.2 ± 4.1	4.18 ± 1.58	1.18 ± 0.58	0.22	0.10 ± 0.10
NGC0024	71.3 ± 1.1	66.5 ± 3.1	35.49 ± 4.46	6.03 ± 2.99	0.21	1.00 ± 1.00
NGC0100	60.7 ± 4.2	40.9 ± 1.9	2.71 ± 0.59	2.22 ± 0.85	0.23	0.00 ± 0.00
NGC3109	46.1 ± 1.8	34.7 ± 3.2	1.88 ± 0.14	0.42 ± 0.10	0.26	0.00 ± 0.00
NGC3972	83.2 ± 3.3	86.4 ± 8.1	7.08 ± 1.40	1.37 ± 0.92	0.87	0.80 ± 0.60
NGC4183	71.2 ± 1.1	72.2 ± 3.3	5.22 ± 0.72	1.05 ± 0.35	0.87	0.70 ± 0.70
NGC4559*	91.0 ± 2.3	66.1 ± 1.0	2.59 ± 0.36	7.82 ± 0.48	0.67	0.20 ± 0.20
NGC6503	83.9 ± 0.6	64.1 ± 0.6	18.66 ± 0.97	23.58 ± 2.86	0.76	5.50 ± 5.50
UGC00731	43.1 ± 1.0	106.1 ± 32.6	3.02 ± 0.37	0.13 ± 0.03	0.91	0.50 ± 0.50
UGC01230	68.6 ± 2.8	75.5 ± 4.2	4.18 ± 1.00	0.60 ± 0.22	0.78	0.30 ± 0.30
UGC01281	39.7 ± 3.0	36.9 ± 4.5	2.33 ± 0.35	0.56 ± 0.15	0.08	0.00 ± 0.00
UGC04325	55.9 ± 1.4	70.7 ± 6.6	16.85 ± 2.09	1.90 ± 0.73	0.70	4.00 ± 4.00
UGC04499	45.8 ± 2.0	48.6 ± 5.0	2.91 ± 0.52	0.85 ± 0.29	0.91	0.50 ± 0.50
UGC05005*	61.6 ± 3.9	62.7 ± 4.1	0.76 ± 0.18	0.14 ± 0.02	0.78	0.00 ± 0.00
UGC05750	50.1 ± 5.9	55.5 ± 5.6	0.65 ± 0.13	0.14 ± 0.05	1.47	0.05 ± 0.05
UGC06399	55.5 ± 3.3	54.8 ± 5.9	3.46 ± 0.70	0.76 ± 0.32	0.87	0.40 ± 0.30

Table A2. Continuation of **Table A1**. For UGC11914, $\Upsilon_* = 0.3$ fixed.

Galaxy	$\langle v_{rb}^2 \rangle^{1/2}$	$\langle v_{rb}^2 \rangle^{1/2}$	$\rho_h(r_{\min})$	$\rho_b(r_{\min})$	r_{\min}	$\Delta\rho_h$
	[km/s]	[km/s]	[$10^{-2} M_{\odot} \cdot \text{pc}^{-3}$]	[$10^{-2} M_{\odot} \cdot \text{pc}^{-3}$]	[kpc]	[same]
UGC06446	50.0 ± 1.1	64.8 ± 6.9	8.11 ± 1.22	0.64 ± 0.26	0.58	1.15 ± 1.00
UGC06667	53.6 ± 1.7	82.4 ± 18.2	3.89 ± 0.44	0.21 ± 0.06	0.87	0.50 ± 0.40
UGC06917	67.3 ± 2.8	75.9 ± 8.2	3.54 ± 0.56	0.68 ± 0.31	1.74	1.05 ± 0.90
UGC06930	67.7 ± 2.7	74.0 ± 5.6	2.91 ± 0.68	0.66 ± 0.25	1.74	0.70 ± 0.70
UGC07125	38.6 ± 1.4	47.8 ± 5.4	0.83 ± 0.17	0.22 ± 0.09	1.44	0.15 ± 0.15
UGC07151	43.3 ± 1.3	52.2 ± 6.9	11.07 ± 1.95	2.07 ± 1.29	0.50	2.00 ± 2.00
UGC07323	62.6 ± 8.8	56.6 ± 8.7	2.38 ± 0.73	1.20 ± 0.63	0.58	0.10 ± 0.10
UGC07399	63.2 ± 1.5	62.3 ± 5.8	18.63 ± 1.98	2.11 ± 0.92	0.61	4.25 ± 4.00
UGC07524	47.6 ± 0.8	79.1 ± 15.0	2.71 ± 0.22	0.19 ± 0.08	0.35	0.05 ± 0.05
UGC07603	41.4 ± 1.6	32.4 ± 2.8	11.12 ± 1.75	4.07 ± 1.72	0.34	1.00 ± 1.00
UGC07608	42.9 ± 5.6	63.7 ± 25.2	3.88 ± 1.25	0.31 ± 0.13	0.60	0.30 ± 0.30
UGC08286	51.4 ± 0.8	56.3 ± 6.8	11.09 ± 1.27	1.25 ± 0.78	0.47	1.50 ± 1.50
UGC08490	53.4 ± 0.9	45.1 ± 1.9	22.02 ± 2.98	10.43 ± 3.91	0.34	4.00 ± 4.00
UGC10310	43.1 ± 2.9	56.6 ± 8.5	4.05 ± 1.17	0.68 ± 0.30	1.10	1.00 ± 1.00
UGC11914*	197.8 ± 0.7	188.1 ± 1.1	526.8 ± 17.3	421.0 ± 11.1	0.28	165 ± 165
UGC12632	43.3 ± 1.0	63.4 ± 10.7	3.03 ± 0.40	0.25 ± 0.11	0.71	0.40 ± 0.40
UGCA442	38.0 ± 1.0	28.7 ± 2.3	2.66 ± 0.32	1.23 ± 0.34	0.42	0.20 ± 0.20

Table A3. Measured adiabatic invariants $v_{\text{rms}}(1)$ for several fits described in Section 3. Uncertainties are statistical at 68% confidence. A systematic uncertainty, due to galaxies not fully relaxed and to possible dark matter rotation, needs to be added. We do not estimate this systematic uncertainty, but rather rely on the standard deviation of $v_{\text{rms}}(1)$ in this sample of galaxies as an upper bound to the total uncertainty.

Galaxy	Fitted	$v_{\text{rms}}(1)$	$v_{\text{rms}}(1)$	$v_{\text{rms}}(1)$	$v_{\text{rms}}(1)$
	Υ_*	[km/s]	$\Upsilon_* = 0.5$	$\Upsilon_* = 0.2$	$m_h = 53.5 \text{ eV}$
D631-7	0.32 ± 0.14	1.27 ± 0.16	1.30 ± 0.18	1.19 ± 0.15	0.99 ± 0.16
DDO064	0.44 ± 0.14	0.55 ± 0.14	0.59 ± 0.16	n.a.	0.66 ± 0.09
DDO161	0.29 ± 0.14	1.47 ± 0.09	1.54 ± 0.09	1.44 ± 0.08	1.40 ± 0.09
ESO116-G012	0.42 ± 0.17	1.03 ± 0.13	1.10 ± 0.07	0.91 ± 0.04	0.77 ± 0.07
F563-1	0.33 ± 0.14	1.00 ± 0.10	1.01 ± 0.11	1.00 ± 0.10	0.83 ± 0.09
F563-V2	n.a.	n.a.	0.85 ± 0.12	0.83 ± 0.11	n.a.
F568-1	0.19 ± 0.09	1.08 ± 0.12	1.04 ± 0.12	1.07 ± 0.12	0.84 ± 0.09
F568-3	0.28 ± 0.13	1.38 ± 0.11	1.43 ± 0.12	1.36 ± 0.10	1.20 ± 0.13
F568-V1	0.30 ± 0.19	0.86 ± 0.10	0.84 ± 0.10	0.87 ± 0.10	0.68 ± 0.06
F571-8	n.a.	n.a.	n.a.	1.57 ± 0.09	n.a.
F574-1	n.a.	n.a.	0.94 ± 0.06	0.91 ± 0.06	n.a.
F579-V1	0.28 ± 0.14	0.63 ± 0.07	0.64 ± 0.08	0.63 ± 0.07	0.57 ± 0.04

Continued

F583-1	0.27 ± 0.08	1.02 ± 0.08	1.03 ± 0.08	1.01 ± 0.07	0.83 ± 0.05
F583-4	0.40 ± 0.15	0.64 ± 0.12	0.67 ± 0.13	0.60 ± 0.09	0.66 ± 0.09
NGC0024	0.26 ± 0.13	0.55 ± 0.03	0.60 ± 0.03	0.54 ± 0.02	0.54 ± 0.03
NGC0100	0.43 ± 0.13	1.12 ± 0.16	1.19 ± 0.11	0.94 ± 0.06	0.84 ± 0.12
NGC3109	0.40 ± 0.15	0.96 ± 0.06	0.98 ± 0.06	0.94 ± 0.05	0.81 ± 0.03
NGC3972	0.22 ± 0.14	1.08 ± 0.12	1.22 ± 0.16	1.07 ± 0.10	0.79 ± 0.07
NGC4183	0.20 ± 0.08	1.01 ± 0.08	1.16 ± 0.11	1.01 ± 0.07	0.91 ± 0.09
NGC4559	n.a.	n.a.	1.67 ± 0.13	1.07 ± 0.05	1.77 ± 0.21
NGC6503	0.29 ± 0.03	0.75 ± 0.09	0.83 ± 0.12	0.72 ± 0.07	0.77 ± 0.12
UGC00731	0.42 ± 0.14	0.73 ± 0.07	0.73 ± 0.07	0.73 ± 0.07	0.63 ± 0.05
UGC01230	0.41 ± 0.14	1.07 ± 0.13	1.08 ± 0.13	1.07 ± 0.14	0.99 ± 0.13
UGC01281	0.48 ± 0.12	0.77 ± 0.10	0.78 ± 0.10	n.a.	n.a.
UGC04325	0.38 ± 0.15	0.52 ± 0.06	0.53 ± 0.06	0.52 ± 0.06	0.46 ± 0.08
UGC04499	0.40 ± 0.15	0.78 ± 0.10	0.81 ± 0.10	0.75 ± 0.08	0.66 ± 0.07
UGC05005	n.a.	n.a.	1.85 ± 0.30	1.74 ± 0.25	n.a.
UGC05750	0.38 ± 0.14	1.45 ± 0.27	1.50 ± 0.28	1.39 ± 0.25	1.28 ± 0.30
UGC06399	0.39 ± 0.15	0.91 ± 0.12	0.94 ± 0.13	0.87 ± 0.10	0.74 ± 0.07

Table A4. Continuation of Table A3. For UGC11914, $\Upsilon_* = 0.3$ fixed.

Galaxy	Fitted	$v_{\text{rms}}(1)$	$v_{\text{rms}}(1)$	$v_{\text{rms}}(1)$	$v_{\text{rms}}(1)$
	Υ_*	[km/s]	$\Upsilon_* = 0.5$	$\Upsilon_* = 0.2$	$m_p = 53.5 \text{ eV}$
UGC06446	0.35 ± 0.14	0.61 ± 0.05	0.62 ± 0.06	0.61 ± 0.05	0.57 ± 0.04
UGC06667	0.44 ± 0.14	0.84 ± 0.07	0.84 ± 0.07	0.84 ± 0.07	0.71 ± 0.04
UGC06917	0.40 ± 0.15	1.04 ± 0.15	1.07 ± 0.16	1.01 ± 0.12	0.85 ± 0.12
UGC06930	0.37 ± 0.14	1.14 ± 0.17	1.18 ± 0.19	1.09 ± 0.14	1.03 ± 0.18
UGC07125	0.32 ± 0.15	1.00 ± 0.13	1.08 ± 0.15	0.96 ± 0.10	0.75 ± 0.08
UGC07151	0.31 ± 0.16	0.47 ± 0.05	0.50 ± 0.06	0.46 ± 0.04	0.55 ± 0.10
UGC07323	0.36 ± 0.15	1.19 ± 0.29	1.40 ± 0.35	1.05 ± 0.15	0.85 ± 0.14
UGC07399	0.37 ± 0.15	0.57 ± 0.06	0.58 ± 0.06	0.56 ± 0.06	0.54 ± 0.06
UGC07524	0.21 ± 0.11	0.87 ± 0.04	0.90 ± 0.04	0.87 ± 0.04	0.71 ± 0.03
UGC07603	0.40 ± 0.14	0.47 ± 0.05	0.48 ± 0.04	0.44 ± 0.03	0.52 ± 0.31
UGC07608	0.39 ± 0.15	0.69 ± 0.17	0.69 ± 0.17	0.68 ± 0.16	0.68 ± 0.12
UGC08286	0.35 ± 0.18	0.57 ± 0.04	0.59 ± 0.04	0.55 ± 0.03	0.55 ± 0.04
UGC08490	0.47 ± 0.14	0.47 ± 0.04	0.47 ± 0.04	0.43 ± 0.03	0.44 ± 0.04
UGC10310	0.40 ± 0.15	0.65 ± 0.13	0.66 ± 0.13	0.63 ± 0.11	0.55 ± 0.11
UGC11914*	n.a.	n.a.	n.a.	0.58 ± 0.06	n.a.
UGC12632	0.36 ± 0.16	0.74 ± 0.06	0.75 ± 0.07	0.73 ± 0.06	0.62 ± 0.04
UGCA442	0.40 ± 0.15	0.69 ± 0.05	0.69 ± 0.05	0.68 ± 0.05	0.56 ± 0.04